

AD-A194 697

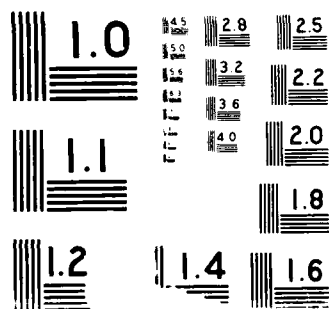
CRITICAL CONDITIONS FOR FAILURE IN MATERIALS SUBJECTED  
TO HIGH RATES OF L (U) BROWN UNIV PROVIDENCE RI DIV OF  
ENGINEERING R J ASARO ET AL 28 MAR 88 ARO-22306 12-EG  
DAGG29-85-K-0003

1/1

UNCLASSIFIED

F/G 11/6 1 NL





AD-A194 697

CRITICAL CONDITIONS FOR FAILURE IN MATERIALS  
SUBJECTED TO HIGH RATES OF LOADING

Final Technical Report

R. J. Asaro, R. J. Clifton (P.I.), J. Duffy,  
L. B. Freund, and A. Needleman

28 March 1988

U. S. ARMY RESEARCH OFFICE

Research Agreement No. DAAG29-85-K-0003

Division of Engineering  
Brown University  
Providence, RI 02912

Approved for public release.  
Distribution unlimited.

DTIC  
ELECTE  
MAY 11 1988  
S  $\alpha$  H D

UNCLASSIFIED

SECURITY CLASSIFICATION OF THIS PAGE

ADA194697

## REPORT DOCUMENTATION PAGE

1a. REPORT SECURITY CLASSIFICATION Unclassified			1b. RESTRICTIVE MARKINGS		
2a. SECURITY CLASSIFICATION AUTHORITY			3. DISTRIBUTION/AVAILABILITY OF REPORT Approved for public release; distribution unlimited.		
2b. DECLASSIFICATION/DOWNGRADING SCHEDULE					
4. PERFORMING ORGANIZATION REPORT NUMBER(S)			5. MONITORING ORGANIZATION REPORT NUMBER(S) AR6 22306.12-EG		
6a. NAME OF PERFORMING ORGANIZATION Brown University		6b. OFFICE SYMBOL (If applicable)		7a. NAME OF MONITORING ORGANIZATION U. S. Army Research Office	
6c. ADDRESS (City, State, and ZIP Code) Box D, Division of Engineering Providence, RI 02912		7b. ADDRESS (City, State, and ZIP Code) P. O. Box 12211 Research Triangle Park, NC 27709-2211			
8a. NAME OF FUNDING/SPONSORING ORGANIZATION U. S. Army Research Office		8b. OFFICE SYMBOL (If applicable)		9. PROCUREMENT INSTRUMENT IDENTIFICATION NUMBER DAA629-85-K-0003	
8c. ADDRESS (City, State, and ZIP Code) P. O. Box 12211 Research Triangle Park, NC 27709-2211		10. SOURCE OF FUNDING NUMBERS			
		PROGRAM ELEMENT NO.		PROJECT NO.	
		TASK NO.		WORK UNIT ACCESSION NO.	
11. TITLE (Include Security Classification) Critical Conditions for Failure in Materials Subjected to High Rates of Loading					
12. PERSONAL AUTHOR(S)					
13a. TYPE OF REPORT Final		13b. TIME COVERED FROM 12/1/84 TO 12/31/87		14. DATE OF REPORT (Year, Month, Day) 1988 March 28	
15. PAGE COUNT 23					
16. SUPPLEMENTARY NOTATION The view, opinions and/or findings contained in this report are those of the author(s) and should not be construed as an official Department of the Army position, policy, or decision, unless so designated by other documentation.					
17. COSATI CODES			18. SUBJECT TERMS (Continue on reverse if necessary and identify by block number)		
FIELD	GROUP	SUB-GROUP	Shear bands, adiabatic shear, dynamic fracture, dynamic plasticity, strain-rate sensitivity, thermal softening, AISI 4340 VAR steel, AISI 1020 steel.		
19. ABSTRACT (Continue on reverse if necessary and identify by block number)					
<p>Dynamic shear band formation in steels has been investigated in torsional Kolsky bar experiments. Temperature profiles have been measured. Stress-time curves have been related to analytical predictions of localization in simple shear. Good agreement between theory and experiment is obtained when the effects of strain hardening, thermal softening, strain rate sensitivity, and geometric imperfections are included in the theory. The analysis of shear strain localization has been extended to the case of plane strain compression. Heat conduction has been included in the analysis of quasi-static deformations.</p> <p>Critical conditions for dynamic and quasi-static fracture initiation of AISI 1020 steel have been determined for three microstructures over the temperature range -150C to +150C. Fracture models for both cleavage fracture and ductile rupture have been</p>					
20. DISTRIBUTION/AVAILABILITY OF ABSTRACT <input type="checkbox"/> UNCLASSIFIED/UNLIMITED <input type="checkbox"/> SAME AS RPT <input type="checkbox"/> DTIC USERS			21. ABSTRACT SECURITY CLASSIFICATION Unclassified		
22a. NAME OF RESPONSIBLE INDIVIDUAL			22b. TELEPHONE (Include Area Code)		22c. OFFICE SYMBOL

developed for interpreting the observed behavior over the full range of temperatures and loading rates. The effect of loading rate on the fracture toughness of 4340 VAR steel has been investigated through experiments involving explosive loading of notched tensile bars and through plate impact experiments on pre-cracked plates. Numerical methods have been developed for the interpretation of the plate impact experiments. Analytical methods have been developed for understanding the effects of strong strain-rate sensitivity on dynamic crack propagation.



Accession For		
NTIS GRA&I	<input checked="" type="checkbox"/>	
ETIC TAB	<input type="checkbox"/>	
Unannounced	<input type="checkbox"/>	
Justification		
By		
Distribution/		
Availability Codes		
Avail and/or		
Dist	Special	
A-1		

## 1. STATEMENT OF PROBLEM

Mathematical models for describing the failure of materials at high rates of loading are inadequate for computing the response of structures subjected to such loading. For example, improved models are required for describing the development of bands of localized shearing deformation ("shear bands") which form in thick steel plates when these plates are impacted by projectiles. Improved models are required also for describing the fracture of metals under impact loading conditions. Such models should be based on a firm understanding of the failure mechanisms in order to determine which material properties must be measured to predict the response of the structure over its range of loading conditions. Furthermore, a mechanistic understanding is required in order to guide the development of new materials and microstructures with improved properties at high loading rates.

Under this research agreement, this overall problem has been addressed by five faculty investigators who have investigated critical conditions for dynamic fracture initiation and for the formation of shear bands. These investigations have been supplemented by investigations of the plastic response of metals at the high strain rates that occur in shear bands and in crack-tip zones. Analytical and computational approaches have been developed to interpret the various experiments and to provide understanding for the development of mechanistic models for computing the failure of structures subjected to high-rate loading.

Research results obtained under the agreement are described in the following section. References without superscripts refer to publications, reports and theses that were supported by the current grant; these publications are listed in Section 2.4. References not supported by the grant are denoted by superscripts R, e.g. (1987)<sup>R</sup>, and listed in Section 2.5.

## 2. SUMMARY OF IMPORTANT RESULTS

### 2.1 Shear Bands

#### 2.1.1 Experiments

A torsional Kolsky bar (split-Hopkinson bar) has been used to deform tubular specimens of four steels (cold rolled AISI 1018, hot rolled AISI 1010, 4340 VAR, and HY-100) at strain rates of  $10^3 \text{ s}^{-1}$  [HARTLEY, DUFFY and HAWLEY, 1987]. Shear bands have been observed to form in all of these steels. The temperature of the material in the bands has been measured by monitoring the infrared radiation emitted at the metal surface. A linear array of ten indium-antimonide detectors has been used to monitor the temperature history at ten neighboring points across the gage section of the specimen. For the relatively wide ( $150\mu\text{m}$ ) shear bands obtained for the AISI 1018 and AISI 1020 steels the maximum temperature rise in the band is approximately  $450^\circ\text{C}$ . This value agrees well with the temperature rise estimated for adiabatic deformation of the material to the shear-band strains observed through the distortion of a grid copied onto the specimen. The shear strains at localization are approximately 15% for the cold rolled steel and 100% for the hot rolled steel. This large difference in the critical nominal strains at localization is consistent with predictions that account for the much greater strain hardening observed for the hot rolled steel.

In order to measure the temperature increases in the relatively narrow bands ( $\approx 10\mu\text{m}$ ) obtained for the 4340 VAR and HY-100 steels, the infrared detection system was improved to minimize aberrations. With this improvement, and with spot sizes of  $35\mu\text{m}$ , temperature increases up to  $600^\circ\text{C}$  have been recorded. From the strains estimated by observing the distorted grids, the estimated temperatures in the shear bands are expected to be larger than the recorded values. This discrepancy is

attributed to the lack of sufficiently fine resolution in the infrared detection system to allow the accurate measurement of temperature over such narrow bands. Availability of these temperature measurements, combined with new high-speed photographs of the developing shear band, has enabled us to establish that the formation of the intensely localized shear band coincides with the sharp decrease in the torque transmitted through the specimen. The critical strain at which the drop in load carrying capacity occurs varies from specimen to specimen in a manner that appears to be consistent with the predicted effects of geometric imperfections on shear strain localization in simple shear [MOLINARI and CLIFTON, 1987].

### 2.1.2 Theory

Shear band formation during simple shearing of thermoviscoplastic materials has been investigated by means of either closed form or essentially closed form solutions of a simplified model problem. In the model problem, inertia, heat conduction, and elastic deformations are neglected. Full numerical solutions have shown that these effects are essentially negligible for the strain rates, specimen sizes, and materials used in the torsional Kolsky bar experiments. Previously, MOLINARI and CLIFTON (1983)<sup>R</sup> had shown that, for the model problem, and for several elementary constitutive models, simple analytical expressions could be obtained for the critical conditions of strain rate sensitivity, thermal softening and strain hardening for which shear localization would occur for sufficiently large strains. These results have been extended to account for geometric and/or material imperfections. For given imperfections the critical nominal shear strain at localization has been obtained either in closed form or in the form of integrals that are relatively easy to evaluate [MOLINARI and CLIFTON, 1987]. Wall thickness variations of specimens used in the torsional Kolsky bar experiments have been measured and used in the prediction of the relationship between the nominal shear stress and the nominal shear strain during

shear band formation. These predicted "stress-strain curves" show good qualitative agreement with those measured in experiments; quantitative agreement is sufficiently close to indicate that accurate measurement of geometrical imperfections of specimens is important in making detailed comparisons between theory and experiment in shear band experiments.

Investigation of the effects of strain hardening, strain-rate sensitivity, thermal softening, heat conduction and the imposed strain rate on the shear localization process has been extended to the case of plane strain compression [LEMONDS and NEEDLEMAN, 1986a]. The deformation, stress and temperature fields are computed in an infinite solid which contains a periodic rectangular array of inhomogeneities. The inhomogeneities give rise to non-uniform deformation fields which may localize in the form of a shear band. Because these fields are periodic, only a rectangular region surrounding a single inhomogeneity needs to be considered. Full two-dimensional, finite element computations are performed within the context of a viscoplasticity theory which, in the rate independent limit, corresponds to flow theory with combined isotropic and kinematic hardening. Full account is taken of finite strain and rotation effects, but attention is confined to quasi-static loading. The predicted response depends significantly on the multi-axial hardening characterization of the solid. The initiation and propagation of shear bands is much more pronounced for the limiting case of kinematic hardening than for the other limiting case of isotropic hardening. This difference in the susceptibility of various model materials to shear band formation is viewed as an indication that constitutive models involving flow potentials with large curvature near the current stress state (as for corner theories in rate independent plasticity) are models for which predictions of shear strain localization are more likely.

In order to develop a better understanding of the effects of thermal softening and heat conduction in shear localization, these effects are included in the analysis of localization in an infinite band [LEMONDS and NEEDLEMAN, 1986b]. Full account is taken of finite geometry changes, but inertial effects are neglected. An energy balance is written between homogeneously deforming bands in a manner that models conditions in the above finite element study of shear band development. The infinite band analysis requires specification of an imperfection amplitude and a length scale over which heat conduction effects are significant. These are chosen to match results of the finite element analysis. The predictions of the band analysis and the full finite element computations are then compared for a wide range of material properties for both isotropic and kinematic hardening characterizations of the flow potential surface. The predicted dependence of the onset of localization on material properties, such as strain hardening and strain-rate sensitivity, is the same for both types of analyses.

The effects of inertia on shear band development in plain strain compression have been investigated for an elastic-viscoplastic material with softening introduced through a hardness function that exhibits a local maximum [NEEDLEMAN, 1987]. An initial inhomogeneity is introduced to cause the deformation to be non-uniform. Regardless of whether the material is hardening or softening, plastic strain development involves the evolution of finger-like contours emanating from the inhomogeneity at  $45^\circ$  to the compression axis. Once a given strain contour crosses the specimen, it fans out about its initial direction of propagation. For a softening solid, this fanning out ceases for some strain level greater than the strain at the hardness maximum and further straining takes place in an ever narrowing band. Many of the qualitative features of shear band development under dynamic loading conditions are the same as under quasi-static loading conditions, but a significant retardation of shear band development due to inertial effects is found.

## 2.2 Dynamic Fracture

### 2.2.1 Notched Bar Experiments and Interpretation

An investigation has been conducted into the effects of microstructure, loading rate, and temperature on the initiation of plane strain fracture of a plain rate, carbon AISI 1020 steel [COUQUE, ASARO, DUFFY, and LEE, 1987]. Ferrite grain sizes and prior austenite grain sizes were varied by changing the austenitizing temperature and the cooling rates during normalization. Three different microstructures were investigated. Grain size differences in these three microstructures were designed to provide independent variation of each of the grain sizes while varying these sizes by a factor of 2 or more. Fracture toughness tests were conducted using pre-cracked notched round bars loaded in tension. The tests were performed at quasi-static loading rates  $\dot{K}_I = 1 \text{ MPa m}^{1/2}\text{s}^{-1}$ , and at dynamic loading rates  $\dot{K}_I = 2 \times 10^6 \text{ MPa m}^{1/2}\text{s}^{-1}$ . Testing temperatures covered the range from  $-150^\circ\text{C}$  to  $150^\circ\text{C}$  corresponding to fracture initiation modes varying from transgranular cleavage to fully ductile fracture. In addition, Charpy impact tests were conducted over the same range of temperatures. The plastic shearing response of the steels, over this range of temperatures, was obtained through torsion tests at quasi-static shear strain rates of  $\dot{\gamma} = 5.0 \times 10^{-4}\text{s}^{-1}$  and at dynamic shear strain rates of  $\dot{\gamma} = 1.5 \times 10^3\text{s}^{-1}$ .

The measured dependence of fracture toughness on microstructure, loading rate and temperature is shown in Fig. 1. The microstructure T1 has the smallest grain sizes and the microstructure T7 has the largest grain sizes; T9 has the prior austenite grain size of T1 and a ferrite grain size comparable to that of T7. For all three microstructures the temperature dependence of the dynamic fracture toughness  $K_{Id}$  consists of a "lower shelf" at temperatures below room temperature (RT), an "upper shelf" at temperatures above  $100^\circ\text{C}$ , and a transition over a relatively narrow range of temperatures between RT and  $100^\circ\text{C}$ . The temperature dependence of the

quasi-static fracture toughness  $K_{Ic}$  is more complicated. Although for each of the three microstructures  $K_{Ic}$  increases from a low value at 150°C to an apparent "upper shelf" at temperatures above 50°C, the increase is not monotonic and the "two shelf" structure is not clearly delineated. For all microstructures and loading rates, fracture initiation at -150°C occurs by cleavage and fracture initiation at +150°C occurs by ductile rupture processes. The fracture toughness at -150°C is essentially the same for all microstructures and loading rates. At +150°C the fracture toughness increases with increasing loading rate and varies significantly with variations in the microstructures. These variations in fracture toughness for fully ductile fracture processes follow the variations in flow stress with loading rate and microstructure.

In order to get a better understanding of the relationship between the fracture toughness and the micromechanical processes involved in fracture through cleavage and through void growth, the fractured specimens were examined using transmission and scanning electron microscopy. For cleaved surfaces the size distributions of cleavage facets were measured. Dimple size distributions were obtained for surfaces that had separated by void growth and coalescence. These measurements were used with micromechanical fracture models in an attempt to correlate the measured fracture toughnesses with parameters that characterize the microscopic failure processes. For pure cleavage, fracture was assumed to occur when the maximum principal stress exceeds a critical value over a critical distance from the crack tip. The critical distance was taken to be two ferrite grain diameters -- a distance that correlates well with cleavage facet sizes. For fully ductile rupture, fracture was assumed to occur when an equivalent plastic strain exceeds a critical value over a critical distance from the crack tip. The critical strain, obtained from independent tensile tests on notched bars, was taken to be the strain at which void nucleation occurs. The critical distance was taken to be twice the spacing of

fracture initiation sites, e.g. MnS inclusions, pearlite grains, and grain boundary carbide plates. For both crack propagation models the dependence of stress and strain on radial distance from the crack tip was taken from the finite element solutions of McMEEKING, (1977)<sup>R</sup>. Comparison of the calculated and measured fracture toughness values are shown in Table 1. The agreement is quite good, even on the non-monotonic increase in  $K_{Ic}$  with test temperature found for the microstructure T1. This agreement suggests that quantitative micromodeling using a simple fracture model is a promising means of correlating both quasi-static and dynamic fracture toughness with microstructures.

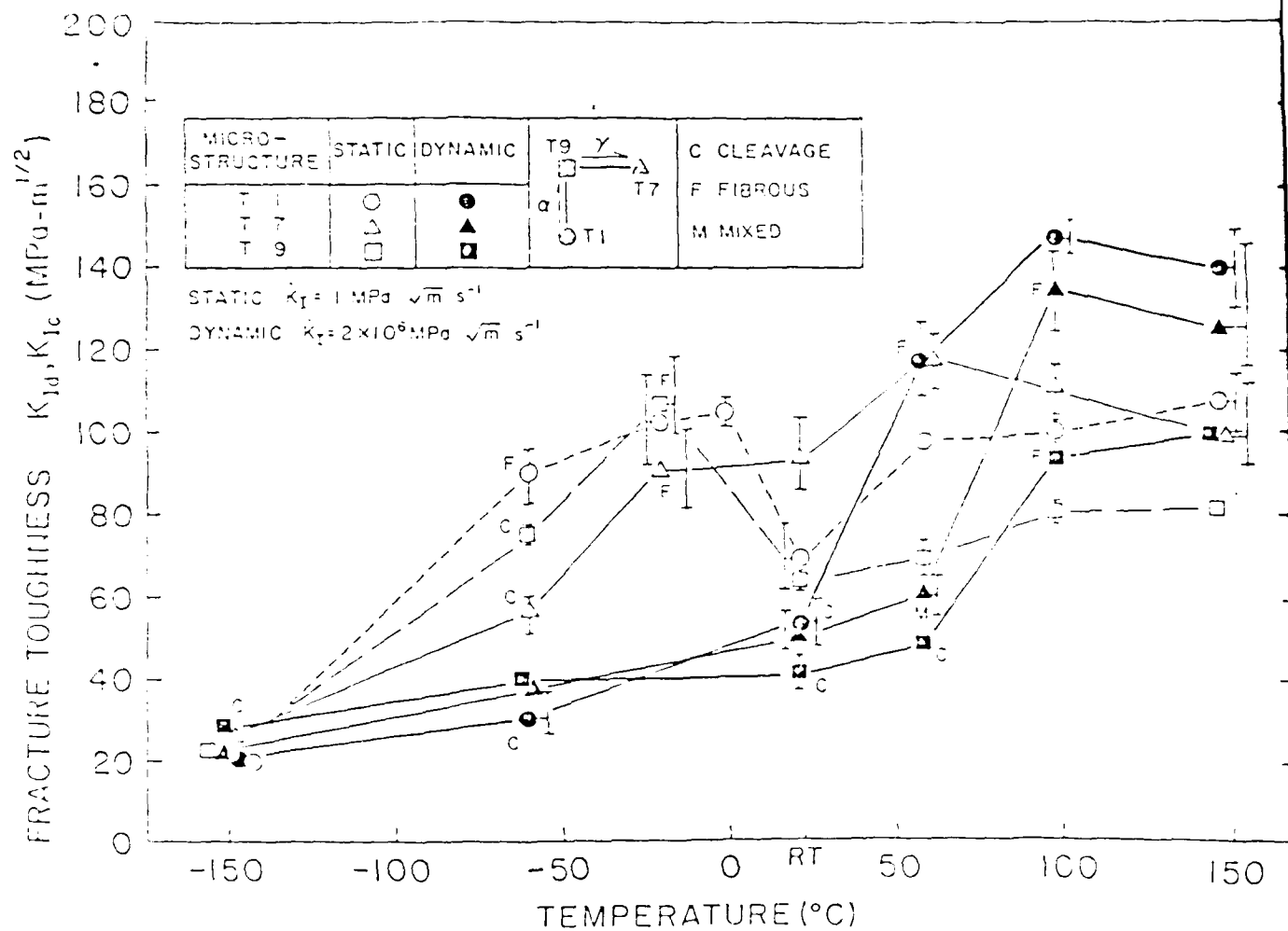


Figure 1: Quasi-static and dynamic values of fracture toughness for the different microstructures as a function of temperature. The fracture initiation mode is indicated qualitatively by the letters 'C', 'F', or 'M' depending upon whether initiation is by cleavage, fibrous, or mixed cleavage-fibrous mechanisms.

Table I      Calculated and measured fracture toughness values.

Loading Condition	Testing Temperature [°C]	T1		T7	
		Calculated $K_{Ic}, K_{Id}$ [Mpa $\sqrt{m}$ ]	Measured $K_{Ic}, K_{Id}$ [Mpa $\sqrt{m}$ ]	Calculated $K_{Ic}, K_{Id}$ [Mpa $\sqrt{m}$ ]	Measured $K_{Ic}, K_{Id}$ [Mpa $\sqrt{m}$ ]
Static	- 150	30 (C)	20 (C)	39 (C)	27 (C)
	- 60	89 (F)	91 (F)	57 (C)	57 (C)
	23	73 (F)	70 (F)	78 (F)	94 (F)
	100	84 (F)	101 (F)	98 (F)	111 (F)
Dynamic	- 150	25 (C)	21 (C)	38 (C)	22 (C)
	- 60	40 (C)	31 (C)	44 (C)	38 (C)
	23	58 (C)	54 (C)	57 (C)	51 (C)
	100	120 (F)	148 (F)	160 (F)	135 (F)

( ) - fracture initiation mode. C; cleavage, F; fibrous.

### 2.2.2 Dynamic Fracture in Plate Impact Experiments

A new plate impact experiment, originated under the previous grant, has been developed for the study of dynamic fracture processes that occur on the sub-microsecond time scale [RAVICHANDRAN and CLIFTON, 1987]. The experiment, designed to make the measurements amenable to interpretation within the framework of fracture mechanics, corresponds to the plane-strain loading of a semi-infinite crack by a step tensile pulse at normal incidence. To obtain these conditions a disc containing a mid-plane, pre-fatigued, edge crack that has been propagated halfway across the diameter is impacted by a thin flyer plate of the same material. A compressive pulse propagates through the specimen and reflects from the rear surface as a square tensile pulse with a duration of  $1\mu\text{s}$ . This plane, tensile pulse causes initiation and propagation of the fatigue crack. The crack advance under the known pulse is measured by using a focussed ultrasonic transducer to locate the crack front before and after the plate impact experiment. Various models for the advance of the crack are examined by prescribing the crack tip motion corresponding to these models and comparing the predicted motion at a point on the rear surface of the specimen with the motion monitored during the experiment using a laser velocity interferometer. All comparisons are made before the experimental results can be affected by the arrival of unloading waves from the periphery of the specimen.

Experiments have been conducted on a hardened 4340 VAR steel ( $R_c = 52$ ) at room temperature and at temperatures of approximately  $-100^\circ\text{C}$ . Crack advance increases with increasing impact velocity and decreasing temperature. The crack paths are quite straight, with essentially no branching; significant turning of the crack towards the rear surface of the specimen occurs at late times. Examination of the fracture surfaces by means of scanning electron microscopy indicates that at room temperature fracture occurs primarily by the ductile process of void initiation, growth

and coalescence whereas at low temperatures fracture occurs by a mixed process involving cleavage across irregularly-shaped regions with a diameter of approximately 10 $\mu$ m combined with ductile rupture of smaller regions between the cleavage facets. The dynamic fracture toughness, represented by the critical value of the stress intensity factor  $K_{Ic}$  required for fracture initiation, is inferred from the corresponding elastodynamic solution and the measured advance of the crack. Values

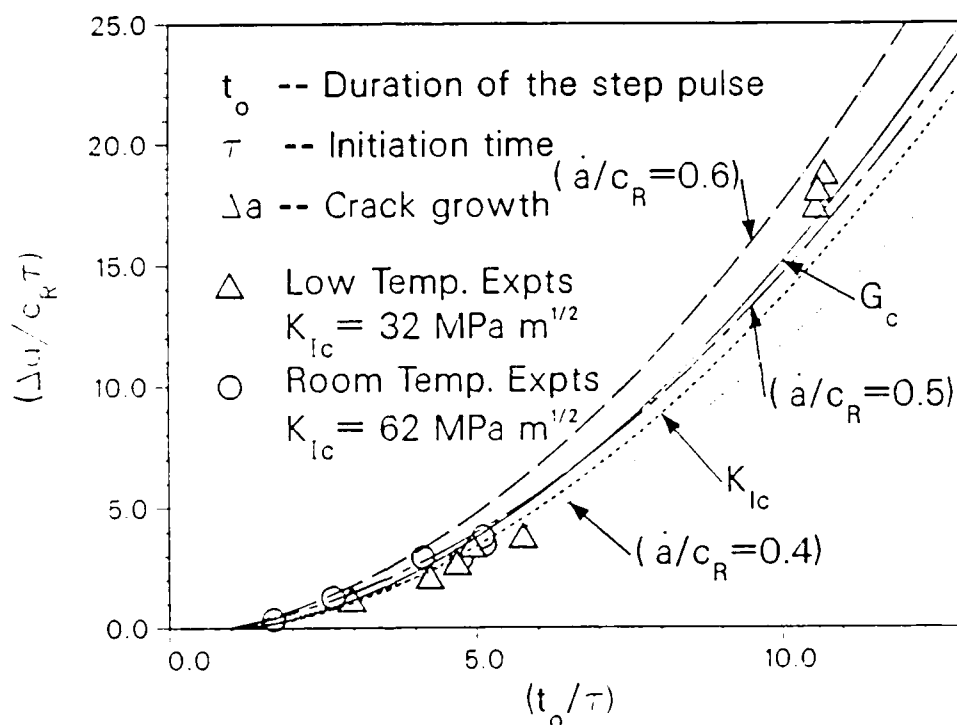


Figure 2 Correlation between measured and predicted crack advances for plate impact experiments on 4340 VAR steel ( $R_s = 52$ ). Predictions are shown for three crack propagation models: (i) constant energy release rate,  $G = G_c$ ; (ii) constant stress intensity factor  $K = K_{Ic}$ ; (iii) constant crack velocity,  $\dot{a}/c_R = 0.4, 0.5, 0.6$ .

of  $K_{Ic} = 62 \text{ MPam}^{1/2}$  and  $K_{Ic} = 32 \text{ MPam}^{1/2}$  are obtained, respectively, for tests at room temperature, and tests at  $-100^\circ\text{C}$ . Essentially the same values are obtained for three different crack propagation models: constant energy release rate, constant stress intensity factor, and constant crack velocity at approximately one-half the Rayleigh wave speed (see Fig. 2); for all models the critical stress intensity factor at crack arrest is assumed to be the same as at crack initiation. The values for  $K_{Ic}$  are higher than interpolated values ( $K_{Ic} = 46$  and  $K_{Ic} = 21$ , respectively) obtained from quasi-static notched bar experiments [CHI, LEE and DUFFY, 1987] on a steel with the same chemical composition. However, the values for  $K_{Ic}$  are lower than the values ( $K_{Ic} = 69$  and  $K_{Ic} = 54$ , respectively) obtained in dynamic notched bar experiments [CHI, LEE, and DUFFY, 1987] at loading rates of  $\dot{K}_I = 10^6 \text{ MPam}^{1/2}\text{s}^{-1}$ . The lower values of  $K_{Ic}$  obtained at the extremely high loading rates (i.e.  $\dot{K}_I = 2 \times 10^8 \text{ MPam}^{1/2}\text{s}^{-1}$ ) of the plate impact experiments have recently been attributed [GODSE, RAVICHANDRAN and CLIFTON, 1988] to the presence of packets of upper bainite which fail by cleavage at load levels below those which cause failure of the fully martensitic microstructure. The presence of upper bainite (up to 15%) results because the plate impact specimens are cut from 2.5-inch diameter bars which are too large to allow the fast quenching at the center that is required to obtain a fully martensitic microstructure.

A second order accurate, finite difference method has been developed for the numerical simulation of these experiments. The loading is modeled as that of a plane, square, tensile pulse impinging at normal incidence on a semi-infinite crack in a plate bounded by two free surfaces. Crack advance is assumed to initiate when the stress intensity factor reaches the critical value  $K_{Ic}$  obtained from correlations with the measured total crack advance. For the low temperature experiments in which the crack-tip plasticity appears to be sufficiently limited to justify the use of linear elastic fracture mechanics, the crack velocities have been prescribed according to the

three different crack propagation models mentioned in the previous paragraph. Although, as noted previously, the value of  $K_{Ic}$  obtained from the measured total crack advance appears to be relatively insensitive to the crack propagation model, the predicted motion at the rear surface is quite sensitive to the crack propagation model. Best agreement with the measured motion at the rear surface, during the motion due to the initial step wave, appears to be obtained for the constant crack velocity model (see Fig. 3). For the room temperature experiments, viscoplastic effects are included in the computations. Reasonable agreement in predicted and measured free surface velocity-time profiles is again obtained when the crack velocity is taken to be constant.

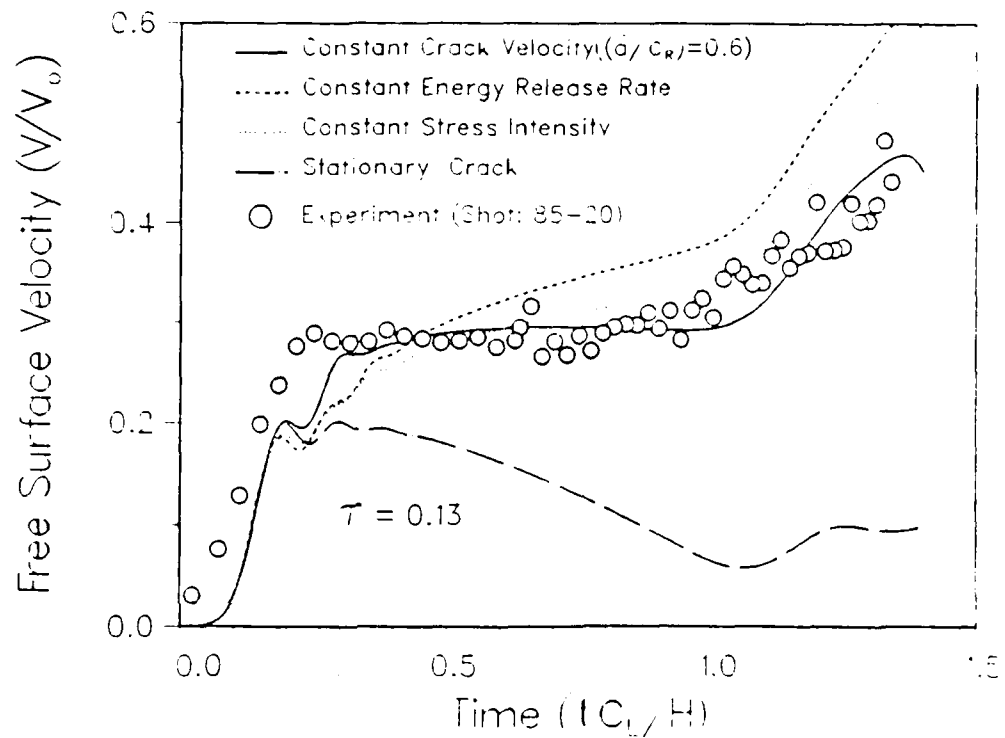


Figure 3 Comparison of measured, free-surface, velocity-time profile for a low temperature ( $-100^{\circ}\text{C}$ ) plate impact experiment with profiles predicted for three crack propagation models: (i) constant energy release rate; (ii) constant stress intensity factor; (iii) constant crack velocity. The predicted velocity-time profile for a stationary crack is included to show the sensitivity of the free surface motion to the motion of the crack.

### 2.2.3 Dynamic Crack Propagation Theory

A model of the high strain rate crack growth process was developed in collaboration with Professor J.W. Hutchinson of Harvard University, based on several observations. First, estimates of material strain rates near the tip of a crack growing in an elastic-plastic material under common conditions suggest that values in the range  $10^4$  -  $10^5$  per second may be anticipated. Experiments on iron conducted at such rates, under more or less homogeneous states of deformation, indicate that the high strain rate response may be divided into two major regimes. For strain rates below a certain level, the flow stress is relatively insensitive to changes in strain rate, whereas above this level the dependence is quite strong. The problem is then studied from the small scale yielding point of view of nonlinear fracture mechanics. Crack growth is assumed to occur in a body that remains elastic at points remote from the crack tip. The applied loading is reflected in a remote stress intensity factor or, equivalently, a rate of energy flux into the crack tip region per unit crack advance. In the crack tip region, the potentially large stresses are relieved to some extent through viscoplastic flow. Thus, crack growth is accompanied by a zone of active plastic deformation and a wake region of permanently deformed but unloaded material along the crack flanks. Within the inner portion of the active plastic zone, where the strain rates are such that the response is in the high rate regime, the stress field is also singular or, equivalently, the rate of energy flux into the crack tip is nonzero. The criterion adopted for sustained cleavage crack growth is that the value of this energy flux must have a certain material specific value. The problem, then, is to determine the influence of the intervening plastic flow in screening the crack tip region from the remotely applied loading. The analysis led to conditions that must be satisfied for sustained steady cleavage crack growth in the materials of interest. The conditions depend on the flow characteristics of the material, the crack tip speed, and the level of applied loading. Of particular

interest is the result that, for given material and temperature, there is a minimum crack driving force below which the propagation of a sharp crack cannot be sustained under any conditions; and this minimum toughness is interpreted as the crack arrest toughness of the material [MATAGA, FREUND, and HUTCHINSON, 1987].

The crack propagation model has also been examined from the dislocation dynamics point of view. The interaction of a rapidly propagating mode I crack with pre-existing dislocations is studied. First, the interaction of a steadily propagating crack with a single edge dislocation near the fracture path is studied. The stress field of the crack induces a shear stress on the glide plane of the dislocation and, if this stress is sufficiently large, the dislocation will move on its glide plane during the interaction. On the basis of a linear viscous drag model for the motion of the dislocation, the energy dissipated in this interaction is computed. The total energy dissipation per unit crack advance is estimated for a distribution of pre-existing dislocations by superposition. The end result is an energy balance that is similar in form to that obtained by the continuum viscoplasticity analysis. This new result, although not exact, permits a re-interpretation of the continuum results in terms of dislocation dynamics concepts.

The foregoing analysis was directed at understanding fracture of those materials that may exhibit strain rate induced cleavage but that fail in a ductile manner under slow loading conditions. Of course, strain rate sensitivity of the material response can also influence the fracture response during crack advance controlled by a ductile separation mechanism. This matter was addressed in a related study in which the problem of steady growth of an antiplane shear crack in a strain rate sensitive elastic-plastic material was considered [YANG and FREUND, 1986]. It was assumed that the material is elastic-perfectly plastic under slow loading

conditions, but that the inelastic strain rate is proportional to the difference between the stress and the yield stress raised to some power. In earlier work on this problem reported by others the possibility of an elastic region in stress space was not considered. They concluded that the asymptotic crack tip field is completely autonomous; however, the local field could not be shown to reduce to a generally accepted rate independent limit as the rate sensitivity of the material vanished. It has been shown in our work that if the possibility of elastic unloading is admitted in the formulation then the asymptotic crack tip solution does indeed approach the correct rate independent limit as the rate sensitivity of the material vanishes. Furthermore, the crack tip field loses the feature of complete autonomy under these conditions. That is, the crack tip field involves a free parameter that can be determined only from the remote fields.

## 2.3 Plasticity at High Strain Rates

### 2.3.1 Pressure-Shear Plate Impact

The high-strain rate pressure-shear plate impact experiment was developed at Brown under previous ARO support. Under the present grant this experiment has been extended to shear strain rates, greater than  $10^6 \text{s}^{-1}$ , which are approximately an order of magnitude larger than those obtained previously. This increase in strain rate has been achieved by developing a lapping procedure that allows specimens to be lapped flat and parallel to thicknesses as small as  $35 \mu\text{m}$  [KLOPP, 1986]. Using this technique S. Huang and R.J. Clifton have conducted a relatively thorough investigation of the strain rate sensitivity of OFHC copper up to strain rates of  $10^6 \text{s}^{-1}$ . The shear stress increases with strain rate over the entire range of strain rates. As one means for understanding this increase, we are developing the capability to change the strain rate during the pressure-shear experiment. Currently, we are trying to reduce the strain rate after approximately  $0.5 \mu\text{s}$  by using a layered

flyer plate consisting of a steel front plate backed by a high-strength aluminum plate. The low impedance aluminum plate causes reflected waves to partially unload the specimen and thereby reduce the strain rate in the specimen. Such experiments are expected to provide important new insight into the relative roles of the strain rate history and the current strain rate in causing the strong increase in flow stress with increasing strain rate at strain rates greater than  $10^4 \text{s}^{-1}$ .

#### 2.4 Publications, Reports and Theses

- |   |      |   |
|---|------|---|
| Chi, Y.C.,<br>Lee, S.H. and<br>Duffy, J.              | 1987 | "The Effects of Tempering Temperature and Test Temperature on the Dynamic Fracture Initiation of AISI 4340 VAR Steel," Brown Univ. Tech. Report (in preparation). |
| Clifton, R.J. and<br>Klopp, R.W.                      | 1985 | "Pressure-Shear Plate Impact Testing," Metals Handbook: Vol. 8 9th Edition, American Society for Metals, pp. 230-239.   |
| Couque, H.  | 1987 | "Correlations of Microstructure with Dynamic and Quasi-Static Fracture in a Plain Carbon Steel," Ph.D. Thesis.  |
| Couque, H., Asaro, R.J.<br>Duffy, J. and<br>Lee, S.H. | 1987 | "Correlations of Microstructure with Dynamic and Quasi-Static Fracture in a Plain Carbon Steel," Brown Univ. Tech. Report (to appear in Met. Trans. A.)           |
| Freund, L.B., Wu, F.-H.<br>and Toullos, M.            | 1985 | "Initiation and Propagation of a Shear Band in Antiplane Shear Deformation", in Plastic Instability, Proc. Considere Memorial Symposium, Paris, pp. 125-134.      |
| Hartley, K.A.   | 1986 | "Temperature Profile Measurement During Shear Band Formation in Steels at High Strain Rates," Ph.D. Thesis.   |
| Hartley, K.A.<br>Duffy, J., and<br>Hawley, R.H.       | 1985 | "The Torsional Kolsky (Split-Hopkinson) Bar," Metals Handbook: Mechanical Testing, Vol. 8, 9th Edition, American Society for Metals, pp. 218-228.                 |
| Hartley, K.A.,<br>Duffy, J. and<br>Hawley, R.H.       | 1987 | "Measurement of the Temperature Profile During Shear Band Formation in Steels Deforming at High Strain Rates," J. Mechs. Phys. of Solids 35, pp. 283-301.         |
| Hawley, R.H.,<br>Duffy, J. and<br>Shih, C.F.          | 1985 | "Dynamic Notched Round Bar Testing," Metals Handbook: Mechanical Testing, Vol. 8 9th Edition American Society for Metals, pp. 275-283.                            |
| Klopp, R.W.<br>Clifton, R.J. and<br>Shawki, T.G.      | 1985 | "Pressure-Shear Impact and the Dynamic Viscoplastic Response of Metals," Mechs. of Matls. 4, pp. 375-385.   |
| Klopp, R.W.   | 1986 | "Plasticity of Aluminum and Iron at High Shear Strain Rate and High Pressure," Ph.D. Thesis.  |
| Lemonds, J.   | 1986 | "Shear Localization in Rate and Temperature Dependent Solids," Ph.D. Thesis.  |

- |   |      |   |
|---|------|---|
| Lemonds, J. and<br>Needleman, A.                      | 1986 | "Finite Element Analyses of Shear Localization in Rate and Temperature Dependent Solids," <i>Meehs. of Mat'ls.</i> 5, pp. 339-361.        |
| Lemonds, J. and<br>Needleman, A.                      | 1986 | "An Analysis of Shear Band Development Incorporating Heat Conduction," <i>Meehs. of Mat'ls.</i> 5, pp. 363-373.                           |
| Mataga, P.A.,<br>Freund, L.B. and<br>Hutchinson, J.W. | 1987 | "Crack Tip Plasticity in Dynamic Fracture," <i>J. Phys. Chem Solids</i> , 48, pp. 985-1005  |
| Molinari, A. and<br>Clifton, R.J.                     | 1987 | "Analytical Characterization of Shear Localization in Thermoviscoplastic Materials," <i>J. of Appl. Meehs.</i> 54, pp. 806-812.           |
| Ravichandran, G.<br>Clifton, R.J.                     | 1986 | "Dynamic Fracture under Plane Wave Loading," Ph.D., Thesis.   |
| Ravichandran, G.<br>Clifton, R.J.                     | 1986 | "Dynamic Fracture under Plane Wave Loading," (to appear in <i>Int'l Journal of Fracture</i> ).  |
| Shawki, T.G.  | 1985 | "Analysis of Shear Band Formation at High Strain Rates and the Visco-Plastic Response of Polycrystals," Ph.D. Thesis.                     |
| Yang, W. and<br>Freund, L.B.                          | 1986 | "An Analysis of Antiplane Shear Crack Growth in a Rate Sensitive Elastic-Plastic Material," <i>Int'l. J. of Fracture</i> 30, pp. 157-174. |
| Needleman, A.   | 1987 | "Dynamic Shear Band Development in Plane Strain," Brown University Technical Report No. 7.  |
| Godse, R.,<br>Ravichandran, G.,<br>and Clifton, R.J.  | 1988 | "Micromechanisms of Dynamic Crack Propagation in an AISI 4340 Steel," Brown Univ. Technical Report No. 8.                                 |
| Freund, L.B.  | 1987 | "Results on the Influence of Crack Tip Plasticity During Dynamic Crack Growth," (to appear in an <i>ASTM STP</i> )                        |

## 2.5 References

- |                                   |      |  |
|-----------------------------------|------|--|
| McMEEKING, R.M.                   | 1977 | J. Mech. Phys. Solids, 25, 357.                        |
| MOLINARI, A. and<br>CLIFTON, R.M. | 1983 | Comptes, Rendus de l'Academie des Sciences,<br>296, 1. |

### 3. Personnel Supported

R.J. Asaro	
R.J. Clifton	
J. Duffy	
L.B. Freund	
A. Needleman	
G. Majda	
Y.C. Chi	Sc.M., June, 1987
H. Couque	Ph.D., June, 1988
S.H. Lee	
R.W. Klopp	Ph.D., June, 1987
K.A. Hartley	Ph.D., June, 1986
W. Tong	Sc.M., June 1988
R.H. Hawley	
J. Lemonds	Ph.D., June, 1987
A. Molinari	
G. Ravichandran	Ph.D., June, 1987
W. Yang	
R. Godse	Ph.D., June, 1988
T. Shawki	Ph.D., June, 1986
P. Rush	
G. Labonte, Jr.	

END

DATED

FILM

8-88

DTIC